Mem. S.A.It. Suppl. Vol. 21, 190


**Memorie** della
**Supplementi**


# Late activity in GRB afterglows. A multidimensional approach.

A. Vlasis[1], Z. Meliani[1,2], R. Keppens[1]

[1] Centre for Plasma Astrophysics, Department of Mathematics, K.U.Leuven, Belgium
[2] Observatoire de Paris, LUTH, F-92190 Meudon, France
e-mail: Alkis.Vlasis@wis.kuleuven.be

**Abstract.**
A late activity of the central engine of Gamma-Ray Bursts (GRBs) followed by energy injection in the external shock has been proposed in order to explain the strong variability which is often observed in multiwavelength observations in the afterglow. We perform high resolution 1D and 2D numerical simulations of late collisions between two ultra-relativistic shells in order to explore these events. We examine the case where a cold uniform shell collides with a self-similar Blandford and McKee shell in a constant density environment and for the 1D case we produce the corresponding on-axis light curves for the afterglow phase investigating the occurrence of optical and radio flares assuming a spherical explosion and a jet scenario with different opening angles. For our simulations we use the Adaptive Mesh Refinement version of the Versatile Advection Code (MPI-AMRVAC) coupled to a linear radiative transfer code to calculate synchrotron emission. We find steeply rising flare like behavior for small jet opening angles and more gradual rebrightenings for large opening angles. Synchrotron self-absorption is found to strongly influence the onset and shape of the radio flare. Preliminary results of the dynamics from the 2D simulation are also presented in this paper.

## 1. Introduction

Within the frameworks of the fireball model (Rees & Mészáros 1994), GRB afterglows have long been accepted to be the result of the deceleration of the external shock in the interstellar medium and the loss of its energy through synchrotron radiation (Zhang & Mészáros 2004). Recent multiwavelength observations however (Burrows et al. 2005; Stanek et al. 2007), exhibit a deviation from this canonical behavior demonstrating a strong variability in afterglow light curves that can not be explained with the standard external shock model.

External medium density enhancements, caused by inhomogeneities of the surrounding medium have been proposed to provide explanation to the appearance of rebrightenings and flares in the afterglow light curves. However, numerical simulations show that even for a large increase of the external medium density this model does not produce sharp features in the light curves (Nakar & Granot 2006; van Eerten et al. 2009).

It has been suggested that a late activity of the central engine producing consecutive explosions after the initial burst could explain the

*Send offprint requests to*: A. Vlasis

observed variability. According to this model a second blast wave propagating in the swept up medium continuously supplies the system with energy refreshing this way the external shock and producing sharp features in afterglow light curves (Falcone et al. 2006; Granot et al. 2003).

## 2. 1D simulation model

We use the 1D special relativistic hydrodynamic equations in spherical coordinates to perform high resolution simulations of the two-shell collision in the afterglow as described in detail in Vlasis et al. (2011). In our model the external shock is described by the Blandford & McKee (BM) self-similar approximation while the second shell is considered as cold and ultrarelativistic. The explosion is assumed to be spherically symmetric and adiabatic. The density of the circumburst medium is considered constant with particle number density $n = 1$ cm$^{-3}$ and pressure given by $p = 10^{-5} n m_p c^2$. The Lorentz factor of the external shock is $\Gamma = 23$ placed in distance $R_0 \simeq 2.04 \times 10^{17}$cm at the beginning of the simulation. The energy of the BM shell is $E = 10^{52}$erg. The second shell is located at distance $\Delta R = 10^{14}$cm behind the BM with initial thickness $\delta = c\Delta t = 3\times10^{13}$cm taking into account a duration $\Delta t = 10^3$s for the second explosion. Lorentz factor and energy of the second shell take the values $2\Gamma/\sqrt{2}$ and $2E$ accordingly.

For the dynamical simulations we are using the Adaptive Mesh Refinement version of the Versatile Advection Code (MPI-AMRVAC) (Keppens et al. 2011; Meliani et al. 2007), and for the light curves the radiation code of van Eerten & Wijers (2009).

The physical properties of the external shock refreshment model require a large computational domain and a very thin second shell which consequently demands very high resolutions. Therefore, we choose a domain of size $[0.01, 10] \times 10^{18}$cm and 240 cells at the coarsest resolution and a maximum level of refinement 22, leading to an effective resolution of $5.03316 \times 10^8$ cells. The front and back of the uniform shell are also forced to higher refinement to prevent numerical diffusion which would cause an artificial spreading of the shell.

In Fig. 1 (upper pictures) we show the evolution of the two-shell system. As the external shock decelerates in the interstellar medium, the forward shock of the second shell catches up, sweeping up matter from the BM shell and increasing its thermal energy. At the same time the second shell is traversed by the reverse shock which results in loosing part of its initial kinetic energy in favor of the thermal. We consider this process to be a strong candidate for explaining the appearance of optical and radio rebrightenings and flares in the afterglow.

For constructing the light curves we consider synchrotron radiation as the main process contributing to the afterglow taking into account the effects of synchrotron self-absorption (ssa) and neglecting Compton scattering and electron cooling that play a negligible role at time and frequencies under consideration. We examine optical and radio light curves assuming different opening angles of the jet. A strong optical rebrightening is observed at time $t_{obs} = 0.2$ days for the spherical explosion case which becomes sharper the smaller the opening angle of the jet is. This can be understood as follows. Early emission time contribution of the synchrotron radiation comes from high emission angles on the jet, therefore the smaller the opening angle of the jet, the less smeared out is a rebrightening in the light curve. Furthermore, a time delay is observed between the optical and radio flare and the reason for this is the ssa mechanism. As the jet is optically thin for optical emission, the contribution of the collision of the two shells in the light curve is obtained as soon as the forward shock of the second shell starts propagating in the BM medium. However, below the self absorption frequency the two-shell system behaves differently. In the radio frequency the jet is optically thick due to ssa and the result of the collision becomes visible only after the collision has completed. Consequently, a sharp peak and a plateau is observed in the optical flare as a result of the heating of the BM matter from the forward shock of the second shell and a sharp peak at the radio flare as soon as the merger of the two shells is completed, as shown in Fig. 1 (lower pictures).

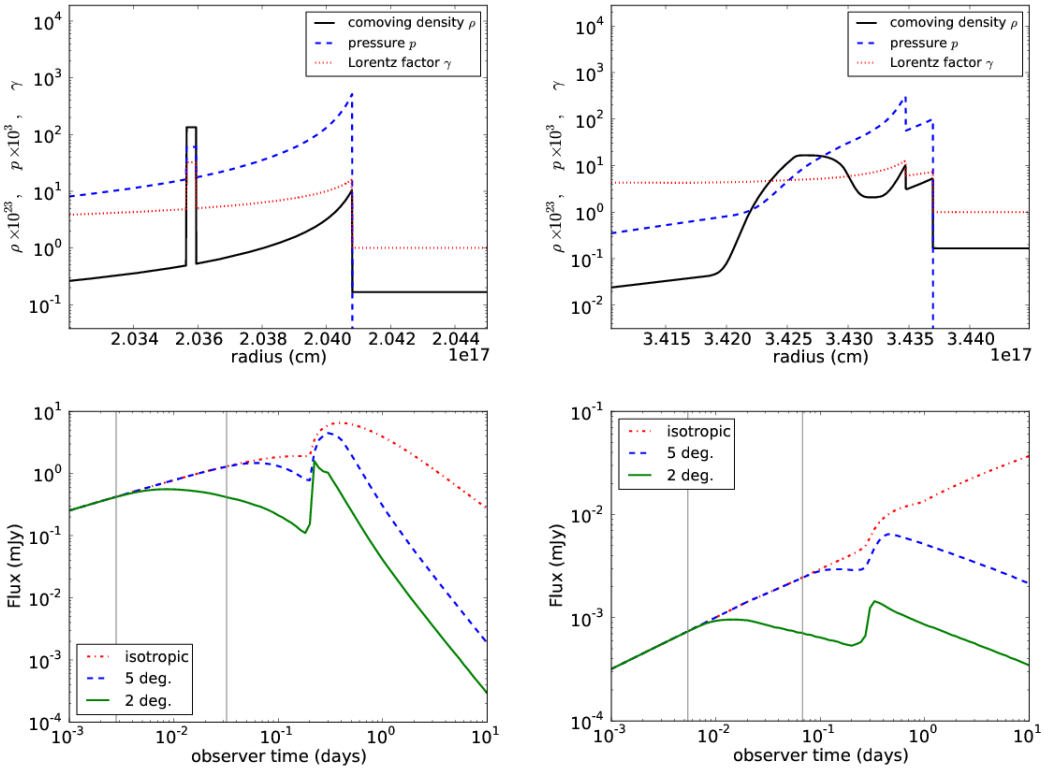


**Fig. 1.** 1D simulation snapshots and light curves. Top figures show the Lorentz factor, density and pressure taken at the initial emission time, $t_e = 6.81 \times 10^6$ sec (left) and at emission time $t_e = 1.15 \times 10^7$ sec (right) at which the forward shock of the second shell is approaching the BM shock. Bottom figures show the optical $5 \times 10^{14}$ Hz (left) and radio $10^8$ Hz (right) light curves assuming different jet opening angle. The jump in the flux density increases the smaller the opening angle of the jet is. Adapted from Vlasis et al. (2011)

## 3. 2D simulation

The validity of the constructed light curves from the 1D simulation requires that the lateral spreading of the jet during the deceleration can be ignored. As shown in Zhang & MacFadyen (2009) the sideways expansion of a jet with opening angle 20 degrees and initial Lorentz factor 20 is a very slow process and starts appearing in times greater than typical afterglow timescales. We perform a 2D numerical simulation of the collision of two shells in the afterglow in order to explore the effects on the dynamical characteristics of the flow originating from the energy injection in the external shock imposing an initial half opening angle of the jet of 2 degrees. The physical properties of the two shells are the same as the ones used in the 1D simulation. We adopt a spherical grid of size $[0.01, 1] \times 10^8$ cm and 4816 cells in the angular direction and $[0, 0.25]$ rad and 28 cells in the angular direction at the coarsest level of refinement. We use a maximum of 10 levels of refinement leading to an effective resolution of $2.46579 \times 10^6$ and 14336 cells in the radial and angular direction respectively. Preliminary results of this simulation are presented in Fig. 2. Close to the origin of the jet the flow is turbulent and dominated by KH instabilities while near the merged shock one can distinguish three dynamically important regions. The merged shock which is charac-

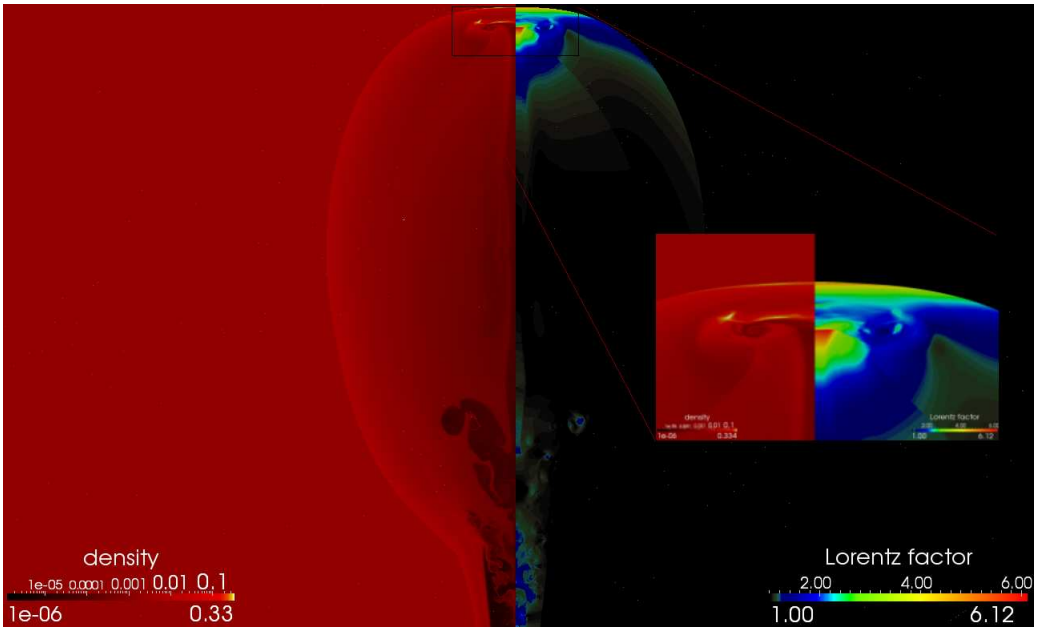


**Fig. 2.** Lorentz factor (right) and comoving density (left) of the jet soon after the collision of the two shocks and a zoom into the region of the shock front.

terized by high comoving density and Lorentz factor and consists of shocked interstellar matter, the remnant of the second shell which after being traversed by the reverse shock has lost most of its initial kinetic energy and the region behind the remnant where the density sharply decreases and the flow accelerates away from the merged shell.

## References

Blandford, R. D., & McKee, C. F. 1976, Phys. Fluids, 19, 1130.
Burrows, D. N. et al. 2005, Sci, 309, 1833
Falcone A. et al. 2006, ApJ, 641, 1010
Granot, J. et al. 2003, Nat., 426, 138
Keppens, R. et al. 2011, J. Comp. Phys., (doi:10.1016/j.jcp.2011.01.020)
Meliani, Z. et al. 2007, MNRAS, 376, 1189
Nakar, E., & Granot, J. 2006, MNRAS, 380, 1744
Rees, M. J., & Mészáros, P. 1994, ApJ, 430, L93
Stanek, K. Z. et al. 2007, ApJ, 654, L21
van Eerten, H. J. et al. 2009, MNRAS, 398, L63
van Eerten, H. J., & Wijers, R. A. M. J. 2009, MNRAS, 394, 2164
Vlasis, A. et al. 2011, MNRAS, 415, 279
Zhang, W., MacFadyen, A. 2009, ApJ, 698, 1261
Zhang, B., & Mészáros, P. 2004, Int. J. Mod. Phys. A, 19,2385